

MetaToken: Detecting Hallucination in Image Descriptions by Meta Classification

Laura Fieback^{1,2}¹Volkswagen AGJakob Spiegelberg¹²Technical University Berlin

{laura.fieback, jakob.spiegelberg}@volkswagen.de

gottschalk@math.tu-berlin.de

Abstract

*Large Vision Language Models (LVLMs) have shown remarkable capabilities in multimodal tasks like visual question answering or image captioning. However, inconsistencies between the visual information and the generated text, a phenomenon referred to as hallucinations, remain an unsolved problem with regard to the trustworthiness of LVLMs. To address this problem, recent works proposed to incorporate computationally costly Large (Vision) Language Models in order to detect hallucinations on a sentence- or subsentence-level. In this work, we introduce **MetaToken**, a lightweight binary classifier to detect hallucinations on the token-level at negligible cost. Based on a statistical analysis, we reveal key factors of hallucinations in LVLMs which have been overseen in previous works. MetaToken can be applied to any open-source LVLM without any knowledge about ground truth data providing a reliable detection of hallucinations. We evaluate our method on four state-of-the-art LVLMs demonstrating the effectiveness of our approach.*

1. Introduction

Recent advances in Large Language Models (LLMs) [4, 7, 51, 59, 71] gave rise to incorporate their few-shot learning capability into vision-language pre-trained models (VL-PTMs) [1, 24, 27, 33, 35, 50, 64] to learn superior cross-modal representations. These models [8, 17, 23, 67, 73], known as Large Vision Language Models (LVLMs), have demonstrated an impressive visual-language understanding by aligning text and visual features. However, besides their remarkable zero-shot performance on visual downstream tasks, LVLMs suffer from the problem of hallucinations [36, 40, 52] inherited from the underlying LLMs or caused by faulty interpretation of the image input by the vision branch.

In the context of LVLMs, hallucination refers to the

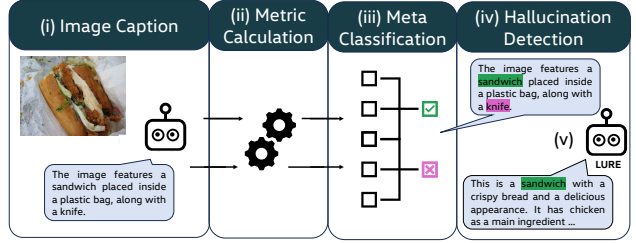


Figure 1. **MetaToken.** Based on generated image captions (i), we calculate our proposed metrics (ii) (see Sec. 3.2). Afterwards, we apply the trained meta classifier (iii) to detect **hallucinated** and **true** objects (iv). Moreover, we show that (v) MetaToken can be easily integrated into LURE [72] to improve the hallucination mitigation.

problem of inconsistencies between the generated text and the visual input [40], diminishing the trustworthiness of these models. Especially in safety-critical applications like autonomous driving [16, 57] or medicine [25, 32], the reliability of the underlying model is indispensable for decision making. In order to address this problem, recent works [9, 15, 19, 19, 30, 62, 66, 70, 72] have proposed additional instruction tuning datasets and pre-training strategies to detect and mitigate hallucinations on a sentence- or subsentence-level. Another common strategy comprises stacked L(V)LMS to post-hoc detect and rectify hallucinations [6, 26, 65, 68].

In this work, we tackle the problem of object hallucination in image captions. To this end, we introduce **MetaToken**, a lightweight hallucination detection method which can be applied to any open-source LVLM. MetaToken builds up on the idea of meta classification [5, 13, 20, 28, 38, 45, 46, 53–55] to detect hallucinated objects on the token-level based on the model output only. Fig. 1 depicts our approach. In contrast to existing methods, our approach neither requires an additional dataset, fine-tuning an L(V)LM nor cost-intensive L(V)LM prompting. Within a

comprehensive statistical analysis, we investigate a broad set of metrics which are indicative of hallucinations providing deep insights into the sources of this specific type of model errors. Our examination reveals key indicators of hallucinations which have not been discovered in previous works. Moreover, our analysis shows that recently identified factors contain less information about hallucinations than our proposed metrics. We evaluate our method on four state-of-the-art LVLMs [8, 23, 67, 73] achieving area under receiver operator characteristic curve values [10] of up to 92.19% and area under precision recall curve values [10] of up to 82.69%. Moreover, we show that our method can be incorporated into the LURE mitigation method [72]. While LURE reduces hallucinations by up to 52.98%, we achieve a hallucination reduction by up to 56.62% through the superior precision-recall-ratio of MetaToken.

To sum up, our main contributions are as follows:

- We propose and investigate a comprehensive set of metrics as potential factors of object hallucinations.
- Based on a statistical analysis, we demonstrate the insufficiency of recently proposed metrics and reveal key factors of object hallucinations.
- Based on these metrics, we introduce MetaToken, a lightweight binary classifier to reliably detect object hallucinations as a post-hoc method. MetaToken can be applied to any open-source LVLM without any knowledge about the ground truth data.
- We show that MetaToken can be easily integrated into the LURE mitigation method, outperforming the initial LURE results through a superior precision-recall-ratio.

2. Related Work

2.1. Large Vision Language Models

VL-PTMs [1, 24, 27, 33, 35, 50, 64] have demonstrated remarkable performance in downstream task by learning universal cross-modal representations [11]. Recent advances in LLMs [4, 7, 51, 59, 71] gave rise to incorporate the few-shot learning capability of LLMs into VL-PTMs. These models [8, 17, 23, 67, 73], known as LVLMs, show an impressive visual-language understanding by aligning visual features with LLMs.

In general, LVLMs can be decomposed into three key components: (i) a vision encoder, which transforms the input image into vision tokens, (ii) a cross-modal alignment network, which aligns the visual and language information and (iii) an LLM, which generates the language output. The training of LVLMs usually consists of (i) the pre-training step using aligned vision-language pairs followed by (ii) vision-language instruction tuning enhancing the zero-shot performance on visual downstream tasks [31]. However, besides their notable success in vision-language tasks, LVLMs suffer from the problem of hallucinations

[36] inherited from the underlying LLMs.

2.2. Object Hallucination

The phenomenon of object hallucination refers to the problem of inconsistencies between the generated text and the visual input [40]. Generally speaking, hallucinations in LVLMs can occur on different semantic levels, where coarse-grained object hallucination [52] refers to objects generated in the language output, which are not depicted in the input image, whereas fine-grained hallucination describes inconsistencies with respect to object attributes or relations between objects [36, 40]. For a comprehensive survey on hallucinations in LVLMs, we refer to [40].

The problem of hallucination mitigation is mainly tackled by either retraining the model with an instruction tuning dataset [15, 19], rectifying image captions as a post-processing step or incorporating new pre-training or generation strategies. LURE [72] serves as a post-hoc method to rectify object hallucinations by training an LVLM-based revisor to reconstruct less hallucinatory descriptions. MARINE [70] enriches the visual context of LVLMs by incorporating object grounding features into the LLM input. In [9], a new pre-training objective is introduced to mitigate object hallucinations by improving the object-level image-text alignment. Motivated by the idea of unlearning, EFUF [66] employs gradient ascent to penalize hallucinations during the unlearning process. Moreover, Visual Contrastive Decoding [30] leverages distorted visual inputs to contrast the output distributions of original and distorted images.

Since the reliability of the generated language output still remains an unsolved problem, many researches focus on the problem of hallucination detection. In [65], the problem of hallucination detection and mitigation is solved simultaneously by raising logical correlated questions and checking for logical consistency throughout the generated answers afterwards. Similarly, Woodpecker [68] serves as a post-processing hallucination detection and correction method incorporating visual knowledge validation for both instance- and attribute-level hallucinations. A human-labeled dataset is published in [19], which is used to train a binary classifier based on the LVLM InstructBLIP [8] to classify between accurate and inaccurate sentences. In [62], an LLM-based hallucination evaluation framework is introduced by training an LLM to distinguish between hallucinated and hallucination-free image captions. Both, [26] and [6], propose a pipeline consisting of several LVLMs and LLMs to verify each claim contained in the generated language output. In this work, we tackle the problem of object hallucination detection by training a lightweight binary classifier. Our method serves as a post-hoc method to classify between true and hallucinated objects. In contrast to existing methods, our approach neither requires an additional dataset, fine-tuning an L(V)LM nor cost-intensive L(V)LM

Table 1. **Related Work on Hallucination Detection.** A comparison of existing approaches on hallucination detection with respect to computational efficiency, i.e., whether the respective method requires an additional dataset, fine-tuning an L(V)LM or prompting an L(V)LM, and the ability of the respective method to detect hallucinations on different semantic levels (hallucination type). ✓ indicates 'yes', ✗ indicates 'no'.

method	computational efficiency			hallucination type		
	w/o add. dataset	w/o fine-tuning	w/o prompting	object	attribute	sentence
LogicCheckGPT [65]	✓	✓	✗	✓	✓	✓
Woodpecker [68]	✓	✓	✗	✓	✓	✓
M-HalDetect [19]	✗	✗	✗	✗	✗	✓
HaELM [62]	✗	✗	✗	✗	✗	✓
FAITHSCORE [26]	✓	✓	✗	✓	✓	✓
UNIHD [6]	✓	✓	✗	✓	✓	✓
Ours	✓	✓	✓	✓	✗	✓

prompting for claim verification (see Tab. 1).

2.3. Meta Classification

In classical machine learning, meta classification refers to the problem of how to best combine predictions from an ensemble of classifiers [38]. In terms of deep learning, this concept has been transferred to the classification whether a prediction is true or false based on uncertainty metrics [20]. Several works have applied this idea to natural language processing [18, 41, 60], image classification [5], semantic segmentation [13, 45, 53, 54], video instance segmentation [46] and object detection [28, 55]. We are the first to transfer the idea of meta classification to the problem of hallucination detection for LVLMs. Based on a statistical analysis of key factors of object hallucination in LVLMs, we identify input metrics outperforming classical uncertainty-based metrics.

2.4. Hallucination Evaluation

Since different studies [9, 52] have shown that standard image captioning metrics like BLEU [49], METEOR [29], CIDEr [61] and SPICE [2] are not capable of measuring object hallucinations properly, most works on hallucination mitigation measure the performance of their proposed method in terms of the Caption Hallucination Assessment with Image Relevance (CHAIR) metric [52]. The CHAIR metric measures the proportion of hallucinated MSCOCO objects [37] in an image caption by matching the MSCOCO objects in the generated text against the ground truth objects provided in the MSCOCO image captioning and object detection datasets [37]. Thus, for every generated MSCOCO object, the CHAIR metric provides a binary label indicating whether the object is true, i.e., contained in the image, or hallucinated. Further datasets and evaluation methods have been proposed to evaluate the performance of LVLMs across multiple multi-modal tasks [14, 15, 19, 21, 36, 39, 42, 43, 62, 63, 69]. While some

of the proposed evaluation methods ask LLMs to output quality-related scores [15, 42, 69] or measure the image-text similarity [21], other methods use a prompt template to query hallucination-related questions and force the model to answer either 'yes' or 'no'. POPE [36] initially proposed to prompt LVLMs with the template '*Is there a <obj> in the image?*' to evaluate the model's performance with respect to object hallucinations. In [14] and [63], this idea is extended by including questions on attribute-level. NOPE [43] comprises negative pronoun data only for different visual question answering tasks. However, the results in [36] and [14] have shown that LVLMs tend to answer 'yes', which results in a low recall for hallucinated objects. Moreover, the LLM- and similarity-based scores [15, 21, 42, 69] evaluate the entire image caption in terms of continuous scores instead of providing a binary label for each generated object. Thus, in this work, we rely on the CHAIR metric to evaluate object hallucinations.

3. Method

The aim of our method is to detect object-level hallucinations [52] in the text output of LVLMs. To this end, we build metrics based on information retrieved from the model output that have been shown to correlate with object hallucinations. These metrics are used to train a lightweight binary meta model to classify between hallucinated and true objects. At inference time, we can detect hallucinations by computing the proposed metrics and applying the trained meta model afterwards.

3.1. Notation

Typically, LVLMs generate language output in an auto-regressive manner by predicting the probability distribution of the next token over the entire vocabulary \mathcal{V} given the input image x , the provided prompt q as well as the already generated tokens. For this purpose, the image x as well as the prompt q are tokenized into $u + 1$ image tokens

t_{x_0}, \dots, t_{x_u} and $v + 1$ prompt tokens t_{q_0}, \dots, t_{q_v} , respectively.

We denote the sequence of generated output tokens by $s = (t_0, \dots, t_K)$ with sequence length $K + 1$. Moreover, let $s_i = (t_0, \dots, t_i)$ denote the generated output sequence at generation step i . The probability of generating token $t_{i+1} \in \mathcal{V}$ at generation step $i + 1$ given the input image x , the provided prompt q and the already generated tokens s_i can then be formulated as $p(t_{i+1}|x, q, s_i)$. For a shorter notation, we define $\hat{p}_{i+1} = p(t_{i+1}|x, q, s_i)$. Furthermore, let p_{i+1} denote the probability distribution at generation step $i + 1$ over the dictionary \mathcal{V} and $|\mathcal{V}|$ the cardinality of \mathcal{V} .

Given the language output s , we can extract all MSCOCO objects [37] contained in the generated text using the CHAIR method [52]. Let $\mathcal{C} = \{c_0, \dots, c_{79}\}$ denote the set of all 80 MSCOCO objects. We denote the set of all MSCOCO objects contained in the sequence s by $\mathcal{O}_s = \{o_0, \dots, o_z\}$ with $o_j \in \mathcal{C}$ for all $j = 0, \dots, z$. Since the generated string of an object might consist of several tokens, we define for every object $o_j \in \mathcal{O}_s$ the start token $t_{o_{j,s}}$ at position $0 \leq o_{j,s} \leq K$ as well as the end token $t_{o_{j,e}}$ at position $0 \leq o_{j,e} \leq K$. Finally, we denote the set of all captions which mention object o_j as \mathcal{S}_{o_j} with cardinality $|\mathcal{S}_{o_j}|$.

3.2. Input Metrics

Recent works [36, 52, 62, 72] have investigated influencing factors of object hallucinations. First, the analysis in [36] has shown that LVLMs are prone to hallucinate objects from the underlying visual instruction tuning datasets. Since the MSCOCO dataset [37] is widely used for instruction tuning, LVLMs tend to hallucinate frequent MSCOCO objects. Furthermore, LVLMs have a high hallucination rate on co-occurring objects, that is, objects which co-occur in the visual instruction tuning datasets frequently tend to occur in the generated language output of LVLMs together even though only one of the objects exists in the image. Thus, we consider the MSCOCO class index (Eq. (1)) which maps a list of synonyms [44] to one of the 80 MSCOCO classes as well as the co-occurrence score (Eq. (2)) inspired from [72]. Second, the results in [62] indicate that LVLMs often generate true segments at the beginning while the risk of hallucinations increases at the latter part of the generated responses. Thus, we take account of the relative position (Eq. (3)) of a generated object and the absolute occurrence (Eq. (4)) of the object in the generated text. Third, to account for the over-reliance of LVLMs on language priors during the generation process [52, 62], we consider the mean absolute attention on the image tokens (Eq. (5)). Finally, we regard the model uncertainty through different dispersion measures (Eq. (7)-(13)) which have been shown to correlate with model errors in different fields [53, 55, 60]. For a generated object $o_j \in \mathcal{O}_s$ from the output sequence

$s = (t_0, \dots, t_K)$, we define

- the **MSCOCO class index**

$$I_{o_j} = k, \quad \text{such that } o_j = c_k, \quad (1)$$

- the **co-occurrence score**

$$H_{o_j} = \sum_{\substack{l=0 \\ o_l \neq o_j}}^z \frac{|\mathcal{S}_{o_l} \cap \mathcal{S}_{o_j}|}{|\mathcal{S}_{o_l} \cup \mathcal{S}_{o_j}|}, \quad (2)$$

- the **relative position**

$$P_{o_j} = o_{j,s}/(K + 1), \quad (3)$$

- the **absolute occurrence** of object o_j in s

$$N_{o_j} = \sum_{l=0}^z \mathbb{1}_{\{o_l = o_j\}}, \quad (4)$$

- for every attention head $g = 0, \dots, G-1$, the **mean absolute attention** of the start token $t_{o_{j,s}}$ on the image tokens t_{x_0}, \dots, t_{x_u}

$$A_{o_j}^g = \frac{1}{u+1} \sum_{r=0}^u |Attention_{t_{o_{j,s}}}(t_{x_r})|, \quad (5)$$

where $Attention_{t_i}(t_n)$ denotes the attention of the generated token t_i at generation step i on the input token t_n ,

- the **log probability**

$$L_{o_j} = \sum_{i=o_{j,s}}^{o_{j,e}} \log \hat{p}_i, \quad (6)$$

- the **cumulated log probability**

$$C_{o_j} = \sum_{i=0}^{o_{j,e}} \log \hat{p}_i, \quad (7)$$

- the sequence **score**¹ with *length_penalty* parameter l_p

$$S_{o_j} = \frac{1}{(o_{j,e})^{l_p}} \sum_{i=0}^{o_{j,e}} \log \hat{p}_i, \quad (8)$$

- the **variance**

$$V_{o_j} = \frac{1}{|\mathcal{V}|} \sum_{t \in \mathcal{V}} (\log p_{o_{j,s}}(t) - \mu)^2 \quad (9)$$

with $\mu = \frac{1}{|\mathcal{V}|} \sum_{t \in \mathcal{V}} \log p_{o_{j,s}}(t)$,

¹https://huggingface.co/docs/transformers/main/en/main_classes/text_generation#transformers.GenerationMixin.compute_transition_scores

- the **entropy** [56]

$$E_{o_j} = -\frac{1}{\log |\mathcal{V}|} \sum_{t \in \mathcal{V}} p_{o_{j,s}}(t) \log p_{o_{j,s}}(t), \quad (10)$$

- the **variation ratio**

$$R_{o_j} = 1 - p_{o_{j,s}}(t_{\max}), \quad t_{\max} = \max_{t \in \mathcal{V}} p_{o_{j,s}}(t), \quad (11)$$

- the **probability margin**

$$M_{o_j} = 1 - p_{o_{j,s}}(t_{\max}) + \max_{t \in \mathcal{V} \setminus \{t_{\max}\}} p_{o_{j,s}}(t), \quad (12)$$

- the **probability difference**

$$D_{o_j} = \log p_{o_{j,s}}(t_{\max}) - \log \hat{p}_{o_{j,s}}, \quad \text{and,} \quad (13)$$

- for LVLMs which use the same vision encoder as CLIP [50], the **CLIPScore** [21]

$$CLIP_{o_j} = \max(100 * \cos(\mathcal{E}_x, \mathcal{E}_{Cap_{o_j}}), 0) \quad (14)$$

with the visual CLIP embedding \mathcal{E}_x for image x and the textual CLIP embedding $\mathcal{E}_{Cap_{o_j}}$ for the caption Cap_{o_j} which is defined as "*a photo of a* $\langle o_j \rangle$ ".

Finally, for an object $o_j \in \mathcal{O}_s$, we define the total set of input metrics for general LVLMs as

$$\mathcal{M}_{o_j} = \{I_{o_j}, H_{o_j}, P_{o_j}, N_{o_j}, A_{o_j}^0, \dots, A_{o_j}^{G-1}, L_{o_j}, C_{o_j}, S_{o_j}, V_{o_j}, E_{o_j}, R_{o_j}, M_{o_j}, D_{o_j}\} \quad (15)$$

with cardinality $|\mathcal{M}_{o_j}| = 12 + G$ and for LVLMs that share the visual embedding with CLIP, the extended set of metrics as

$$\mathcal{M}_{o_j}^{\text{clip}} = \{I_{o_j}, H_{o_j}, P_{o_j}, N_{o_j}, A_{o_j}^0, \dots, A_{o_j}^{G-1}, L_{o_j}, C_{o_j}, S_{o_j}, V_{o_j}, E_{o_j}, R_{o_j}, M_{o_j}, D_{o_j}, CLIP_{o_j}\} \quad (16)$$

with cardinality $|\mathcal{M}_{o_j}^{\text{clip}}| = 13 + G$.

3.3. Hallucination Detection

In this section, we assume a general LVLM that uses a vision encoder different from CLIP. In order to detect hallucinations in the generated output s , we train a lightweight binary meta model to classify between true and hallucinated objects. To this end, let

$$f : \mathbb{R}^{12+G} \rightarrow \{0, 1\} \quad (17)$$

denote the binary classifier. We denote our set of training captions by $\mathcal{S}^{\text{train}}$ and the corresponding set of generated objects by

$$\mathcal{O}_{\mathcal{S}^{\text{train}}} = \bigcup_{s \in \mathcal{S}^{\text{train}}} \mathcal{O}_s. \quad (18)$$

Table 2. **Generation Configurations.** The generation configurations applied in our experiments for nucleus sampling [22] and beam search [3], respectively.

parameter	nucleus sampling	beam search
do_sample	True	False
top_p	0.9	0.9
temperature	1	1
num_beams	1	5
max_length	256	256
min_length	1	1
repetition_penalty	1	1.5
length_penalty	1	1

For every object $o_j \in \mathcal{O}_{\mathcal{S}^{\text{train}}}$ we build an input vector $m_{o_j} \in \mathbb{R}^{12+G}$ representing the metric set \mathcal{M}_{o_j} (Eq. (15)) and define the label $y_{o_j} \in \{0, 1\}$ according to the CHAIR evaluation (see Sec. 4.2). After standardizing the inputs, we use the set

$$\{(m_{o_j}, y_{o_j}) \mid j = 0, \dots, |\mathcal{O}_{\mathcal{S}^{\text{train}}}| - 1\} \quad (19)$$

to train the classifier f .

Given a generated caption s at inference time, we calculate the input vector $m_{o_j} \in \mathbb{R}^{12+G}$ for every object $o_j \in \mathcal{O}_s$ and apply the trained binary meta classifier f to detect hallucinated objects. Note that the input vector m_{o_j} can be calculated based on the model output only without any knowledge of the ground truth data.

4. Experimental Settings

4.1. Dataset

The MSCOCO dataset [37] is a large-scale dataset for object detection, segmentation, and image captioning comprising more than 200K labeled images for 80 object categories. Following [36], we randomly sample 5,000 images from the MSCOCO validation set and produce image captions s for four state-of-the-art LVLMs. We use 80% of the generated captions as our training set $\mathcal{O}_{\mathcal{S}^{\text{train}}}$ and validate our method on the remaining 20% denoted as $\mathcal{O}_{\mathcal{S}^{\text{val}}}$. In our experiments, we average our results over ten randomly sampled training-validation splits. In tables, the corresponding standard deviations are given in parentheses.

4.2. Hallucination Evaluation

Given an image caption, the CHAIR method [52] provides a binary label for every generated MSCOCO object and corresponding synonyms [44] indicating whether the object is true, i.e., contained in the image, or hallucinated. The CHAIR metric measures the proportion of hallucinated

MSCOCO objects by matching the generated text against the ground truth objects provided in the MSCOCO image captioning and object detection datasets [37]. It is defined on two semantic levels: The object instance level CHAIR_i to measure the proportion of hallucinated MSCOCO objects in an image caption which is defined as

$$\text{CHAIR}_i = \frac{|\{\text{hallucinated objects}\}|}{|\{\text{all objects mentioned}\}|} \quad (20)$$

as well as the sentence level CHAIR_s to measure the proportion of hallucinated captions defined as

$$\text{CHAIR}_s = \frac{|\{\text{captions with hallucinated objects}\}|}{|\{\text{all captions}\}|}. \quad (21)$$

Since we tackle the problem of object instance hallucinations in generated captions s , we use the CHAIR_i metric to extract all MSCOCO objects $\mathcal{O}_s = \{o_0, \dots, o_z\}$ and simultaneously label the extracted objects as either true, which is encoded as 0, or hallucinated, which is encoded as 1.

4.3. Large Vision Language Models

We evaluate our approach on four state-of-the-art open-source LVLMs, i.e., InstructBLIP (Vicuna-7B) [8], mPLUG-Owl (LLaMA-7B) [67], MiniGPT-4 (Vicuna-7B) [73], and LLaVa 1.5 (Vicuna-7B) [23], all of them using $G = 32$ attention heads. We use nucleus sampling [22] and the prompt

"Describe all objects in the image."

for all image caption generations. For InstructBLIP and mPLUG-Owl, we create further image captions based on beam search [3]. Tab. 2 states the detailed generation configurations of our experiments. The performance of the LVLMs considered with respect to the average number of generated MSCOCO objects per image as well as the hallucination rate in terms of CHAIR_i (Eq. (20)) and CHAIR_s (Eq. (21)) is summarized in Tab. 3. Note that these results highly depend on the respective generation configurations, the underlying LLM (7B vs. 13B), as well as the chosen prompt [36, 62].

4.4. Evaluation Metrics and Meta Models

We evaluate our method based on the accuracy ACC , the area under receiver operator characteristic curve $AUROC$ [10] and the area under precision recall curve $AUPRC$ [10]. The receiver operator characteristic curve illustrates the performance of a binary classifier by plotting the true positive rate against the false positive rate at various decision thresholds indicating the ability to distinguish between both classes. The precision recall curve plots precision values against the recall at various decision thresholds accounting for imbalance in the underlying dataset. Since we observe highly imbalanced data with respect to object instance

Table 3. **LVLM Performance.** Evaluation results of state-of-the-art LVLMs with respect to the average number of generated MSCOCO objects per image (#MSCOCO obj.), CHAIR_i (Eq. (20)) and CHAIR_s (Eq. (21)). (sample) refers to nucleus sampling generation [22], (beam) reflects beam search. The best results in each block are highlighted.

Model	#MSCOCO obj.	$\text{CHAIR}_i \downarrow$	$\text{CHAIR}_s \downarrow$
InstructBLIP (sample)	5.6	10.4	33.6
mPLUG-Owl (sample)	6.9	30.2	71.6
MiniGPT-4 (sample)	4.4	13.6	33.4
LLaVa (sample)	7.3	18.7	59.2
InstructBLIP (beam)	5.1	7.6	25.0
mPLUG-Owl (beam)	6.7	25.3	63.4

hallucinations (see Tab. 3), the main focus in our evaluation is on the $AUROC$ and $AUPRC$ value. We compare two binary meta models, i.e., a classifier based on a logistic regression and a meta model based on gradient boosting.

4.5. Baseline

As previous works on meta classification [47, 53, 54], we use common uncertainty measures as our baseline. In our experiments, we consider the log probability baseline L (Eq. (6)) and the entropy baseline E (Eq. (10)). For both metrics, we train a baseline classifier in the one-dimensional space, i.e.,

$$f^{\text{baseline}} : \mathbb{R} \rightarrow \{0, 1\} \quad (22)$$

with training set $\{(L_{o_j}, y_{o_j}) \mid j = 0, \dots, |\mathcal{O}_{\mathcal{S}^{\text{train}}}| - 1\}$ and $\{(E_{o_j}, y_{o_j}) \mid j = 0, \dots, |\mathcal{O}_{\mathcal{S}^{\text{train}}}| - 1\}$, respectively.

Note that a direct comparison of our approach to the state-of-the-art methods listed in Tab. 1 is not possible. While our method tackles the problem of token-level instance hallucination, the listed methods either evaluate image captions on a sentence- or subsentence-level [19, 62] or based on atomic facts extracted from the image captions [6, 26, 65, 68]. Thus, the proposed methods [19] and [62] do not provide any information on which specific word of the respective sentence or subsentence is hallucinated. Similarly, [6, 26, 65, 68] are based on atomic facts which neither allow for a token-level evaluation. Moreover, the analysis in [26] shows that the atomic fact extraction already induces detection errors propagating through the detection and evaluation pipeline. To overcome these issues, we rely on the handcrafted CHAIR evaluation (see Sec. 4.2) based on the human-labeled MSCOCO dataset.

Table 4. **Experimental Results based on Nucleus Sampling [22].** Hallucination detection results on four state-of-the-art LVLMs with log probability baseline L (Eq. (6)) and entropy baseline E (Eq. (10)). **Ours** refers to the metric set \mathcal{M} (Eq. (15)), while **Ours^{clip}** is based on the extended metric set $\mathcal{M}^{\text{clip}}$ (Eq. (16)). The classifiers based on logistic regression and gradient boosting are denoted by LR and GB, respectively. The best results in each block are highlighted.

		ACC (in %) \uparrow		$AUROC$ (in %) \uparrow		$AUPRC$ (in %) \uparrow	
		LR	GB	LR	GB	LR	GB
InstructBLIP	L	89.46($\pm 1.4e-3$)	89.46($\pm 1.3e-3$)	73.51($\pm 8.7e-3$)	73.16($\pm 9.0e-3$)	27.07($\pm 2.1e-2$)	25.6($\pm 2.5e-2$)
	E	89.49($\pm 1.6e-3$)	89.48($\pm 1.6e-3$)	65.49($\pm 1.3e-2$)	66.23($\pm 1.5e-2$)	15.38($\pm 5.7e-3$)	17.68($\pm 7.0e-3$)
	Ours	91.33($\pm 1.8e-3$)	91.48 ($\pm 1.5e-3$)	89.94($\pm 9.1e-3$)	90.39 ($\pm 6.8e-3$)	56.13($\pm 1.2e-2$)	57.50 ($\pm 1.0e-2$)
mPLUG-Owl	L	72.42($\pm 4.3e-3$)	72.48($\pm 4.6e-3$)	71.75($\pm 9.4e-3$)	71.86($\pm 9.3e-3$)	51.21($\pm 1.2e-2$)	50.65($\pm 1.1e-2$)
	E	70.06($\pm 4.9e-3$)	70.77($\pm 2.9e-3$)	66.01($\pm 6.3e-3$)	68.33($\pm 6.1e-3$)	40.09($\pm 8.2e-3$)	45.54($\pm 1.2e-2$)
	Ours	82.87($\pm 2.7e-3$)	83.56 ($\pm 3.1e-3$)	88.55($\pm 3.7e-3$)	89.87 ($\pm 2.3e-3$)	76.11($\pm 5.8e-3$)	78.61 ($\pm 7.9e-3$)
	Ours^{clip}	85.05($\pm 2.8e-3$)	85.84 ($\pm 2.9e-3$)	91.29($\pm 3.2e-3$)	92.19 ($\pm 2.1e-3$)	80.98($\pm 4.3e-3$)	82.69 ($\pm 6.1e-3$)
MiniGPT-4	L	86.91($\pm 3.6e-3$)	86.85($\pm 3.9e-3$)	67.26($\pm 2.1e-2$)	67.01($\pm 2.1e-2$)	26.25($\pm 1.7e-2$)	25.41($\pm 1.2e-2$)
	E	86.84($\pm 3.6e-3$)	86.82($\pm 3.6e-3$)	60.78($\pm 1.8e-2$)	63.19($\pm 1.2e-2$)	15.77($\pm 6.7e-3$)	18.98($\pm 1.3e-2$)
	Ours	88.92($\pm 3.5e-3$)	89.27 ($\pm 4.9e-3$)	88.16($\pm 1.5e-2$)	89.74 ($\pm 1.3e-2$)	54.90($\pm 6.5e-2$)	57.27 ($\pm 5.7e-2$)
LLaVa	L	81.57($\pm 1.4e-3$)	81.49($\pm 1.6e-3$)	70.53($\pm 8.7e-3$)	70.73($\pm 6.6e-3$)	37.53($\pm 2.0e-2$)	36.59($\pm 1.7e-2$)
	E	81.28($\pm 2.8e-3$)	81.26($\pm 2.9e-3$)	62.73($\pm 9.0e-3$)	64.63($\pm 7.7e-3$)	23.85($\pm 6.3e-3$)	27.52($\pm 4.6e-3$)
	Ours	87.25($\pm 2.0e-3$)	87.78 ($\pm 3.0e-3$)	90.05($\pm 4.0e-3$)	91.01 ($\pm 4.3e-3$)	70.15($\pm 1.0e-2$)	72.58 ($\pm 1.3e-2$)
	Ours^{clip}	87.93($\pm 1.2e-3$)	88.36 ($\pm 1.6e-3$)	91.73($\pm 2.4e-3$)	92.50 ($\pm 2.5e-3$)	73.00($\pm 7.8e-3$)	75.08 ($\pm 8.5e-3$)

Table 5. **Expected Calibration Error.** The ECE for the logistic regression (LR) and gradient boosting (GB) MetaToken classifier.

ECE (in %) \downarrow		
	LR	GB
InstructBLIP	0.81($\pm 3.2e-4$)	1.29($\pm 4.6e-4$)
mPLUG-Owl	1.36($\pm 1.3e-3$)	2.01($\pm 6.9e-4$)
MiniGPT-4	1.35($\pm 9.5e-4$)	1.43($\pm 8.8e-4$)
LLaVa	1.05($\pm 2.0e-4$)	1.38($\pm 8.1e-4$)

5. Results

5.1. Hallucination Detection

In this section, we discuss the performance of our proposed method with respect to ACC , $AUROC$ and $AUPRC$ on four state-of-the-art LVLMs. We evaluate our method for two lightweight meta models, i.e., a logistic regression (LR) and a gradient boosting (GB) classifier. We refer to Appendix A for the configuration details. Tab. 4 summarizes our results. First, we consider the general metric set \mathcal{M} (Eq. (15)) for image captions based on nucleus sampling [22]. We achieve an ACC of up to 91.48%, $AUROC$ values of up to 91.01%, and $AUPRC$ values of up to 78.61% which clearly outperforms the one-dimensional baselines L

(Eq. (6)) and E (Eq. (10)). While the gradient boosting classifier outperforms the linear model for our method in all experiments, this result does not hold for the one-dimensional baselines L and E . Especially for the log probability baseline L , the linear model is superior to the GB classifier in most of the experiments. Tab. 5 states the expected calibration error (ECE) [48] of our method for the LR and GB classifier. Both models provide a statistical reliable classification between true and hallucinated objects.

Moreover, we evaluate our method on the extended metric set $\mathcal{M}^{\text{clip}}$ (Eq. (16)) for the LVLMs sharing the vision encoder with CLIP [50], that is, mPLUG-Owl [67] and LLaVa [23]. The results are included in Tab. 4. The additional CLIPScore metric (Eq. (14)) improves the ACC by up to 2.28pp, the $AUROC$ by up to 2.74pp and $AUPRC$ by up to 4.87pp underlining the informative content provided by the cosine similarity between the image and text embedding. However, note that the CLIPScore metric can only be calculated in a lightweight manner if the objects of interest \mathcal{C} are known in advance (to calculate the text embedding $\mathcal{E}_{Cap_{o_j}}$ for all possible objects $o_j \in \mathcal{C}$ beforehand) and if the CLIP image embedding \mathcal{E}_x is calculated during the generation process. Since our focus is on a general method without any restrictions, we will stick to the more general metric set \mathcal{M} (Eq. (15)) in the next sections.

Table 6. **Experimental Results based on Beam Search [3].** Hallucination detection results for InstructBLIP [8] and mPLUG-Owl [67] with log probability baseline L (Eq. (6)) and entropy baseline E (Eq. (10)). **Ours** refers to the metric set \mathcal{M} (Eq. (15)). The classifier based on logistic regression and gradient boosting are denoted by LR and GB, respectively. The best results in each block are highlighted.

		ACC (in %) \uparrow		$AUROC$ (in %) \uparrow		$AUPRC$ (in %) \uparrow	
		LR	GB	LR	GB	LR	GB
InstructBLIP	L	92.27 $(\pm 1.6e-3)$	92.20 $(\pm 1.7e-3)$	70.68 $(\pm 2.2e-2)$	70.38 $(\pm 1.8e-2)$	21.57 $(\pm 2.9e-2)$	19.59 $(\pm 2.4e-2)$
	E	92.30 $(\pm 1.7e-3)$	92.27 $(\pm 1.7e-3)$	71.25 $(\pm 1.7e-2)$	71.38 $(\pm 1.8e-2)$	23.69 $(\pm 3.5e-2)$	22.05 $(\pm 2.9e-2)$
	Ours	93.08 $(\pm 1.2e-3)$	93.08 $(\pm 1.3e-3)$	89.70 $(\pm 4.3e-3)$	89.94 $(\pm 6.9e-3)$	47.58 $(\pm 4.7e-2)$	48.14 $(\pm 5.0e-2)$
mPLUG-Owl	L	77.64 $(\pm 2.8e-3)$	77.61 $(\pm 3.5e-3)$	72.00 $(\pm 5.6e-3)$	72.72 $(\pm 4.1e-3)$	50.87 $(\pm 8.3e-3)$	50.35 $(\pm 8.3e-3)$
	E	78.47 $(\pm 4.6e-3)$	78.47 $(\pm 4.4e-3)$	72.58 $(\pm 7.5e-3)$	73.62 $(\pm 6.0e-3)$	52.99 $(\pm 1.3e-2)$	52.55 $(\pm 1.2e-2)$
	Ours	84.23 $(\pm 3.5e-3)$	84.89 $(\pm 4.3e-3)$	89.00 $(\pm 3.1e-3)$	90.54 $(\pm 2.9e-3)$	72.02 $(\pm 7.8e-3)$	74.78 $(\pm 9.0e-3)$

Finally, we observe better results with respect to the $AUPRC$ for LVLMs with a higher hallucination rate, like mPLUG-Owl [67] (see Tab. 3). This behavior is expected due to the highly imbalanced datasets for strong LVLMs, that is, models with a low hallucination rate induce less positive (hallucinated) training samples which makes the problem of learning the lightweight classifier f more challenging. Simultaneously, we achieve higher ACC values for stronger LVLMs like InstructBLIP [8] indicating the insufficiency of the accuracy as an evaluation metric for imbalanced datasets. While, for the sake of completeness, we state the performance of our method with respect to the ACC , we emphasise the superior interpretability of the $AUROC$ and $AUPRC$ values for imbalanced datasets [10].

5.2. Beam Search vs. Nucleus Sampling

The results from the previous section also hold for image captions based on beam search. To compare both generation methods, we generate additional image captions using the beam search algorithm for InstructBLIP [8] and mPLUG-Owl [67]. The results are stated in Tab. 6. Again, the best results for our method are obtained by the gradient boosting classifier, clearly outperforming the single-metric baselines L (Eq. (6)) and E (Eq. (10)). As we can see from Tab. 3, beam search (beam) induces less hallucinations than nucleus sampling (sample) which is in line with previous findings [34, 62]. Thus, the resulting classification problem (beam) is more challenging, i.e. in general, we obtain better detection results for the sampling-based captions with respect to $AUROC$ and $AUPRC$ (see Tabs. 4 and 6).

While the log probability baseline L (Eq. (6)) shows similar classification performance for both, nucleus sampling- and beam search-based captions (see Tabs. 4 and 6), the entropy baseline E (Eq. (10)) is more powerful for captions generated with beam search than for sampled descriptions. Even though we observe less hallucinations using the beam search algorithm (see Tab. 3), we obtain better classification

results from the entropy baseline E (beam) than E (sample). To this end, note that the entropy metric E_{o_j} serves as a measure of uncertainty of generating token $t_{o_{j,s}}$ from the dictionary \mathcal{V} (see Sec. 3). Thus, we expect a higher entropy, i.e., a flatter probability distribution over the dictionary for hallucinated objects and a smaller entropy for true objects. In fact, we can see in Figs. 2c and 2f that this holds for both, nucleus sampling and beam search. However, nucleus sampling induces generally smaller log probability values L (sample) (see Figs. 2a and 2d), and thus, a flatter probability distribution over the dictionary than beam search resulting in a smaller variance V (sample) (see Figs. 2b and 2e). Thus, for nucleus sampling, we obtain generally higher entropy values E (sample) which results in a higher overlap of entropy values for true and hallucinated objects (see Fig. 2f), which makes the classification problem more challenging. For further insights we refer to Appendix B.

5.3. Metric Analysis

In this section, we investigate the information contained in our proposed metrics introduced in Sec. 3.2. A visualization of these metrics can be found in Appendix C. We make use of the least absolute shrinkage and selection operator (LASSO) algorithm [12, 58] to analyze the predictive power of the metrics considered. The LASSO method performs a variable selection for a linear regression including the estimation of the corresponding coefficients ranking the most informative metrics. For the attention metrics (Eq. (5)), we use the maximum of the absolute values of all G weight coefficients. The LASSO path based on the image captions obtained from mPLUG-Owl using nucleus sampling is plotted in Fig. 3. The attention metrics $A^g, g = 0, \dots, G-1$ (Eq. (5)) are selected first, closely followed by the absolute occurrence N (Eq. (4)), the log probability L (Eq. (6)) as well as the cumulated log probability C (Eq. (7)). Moreover, the LASSO path indicates a minor relevance of the co-occurrence score H (Eq. (2)), the sequence score S (Eq. (8)) and the variance V (Eq. (9)). We obtain similar results inde-

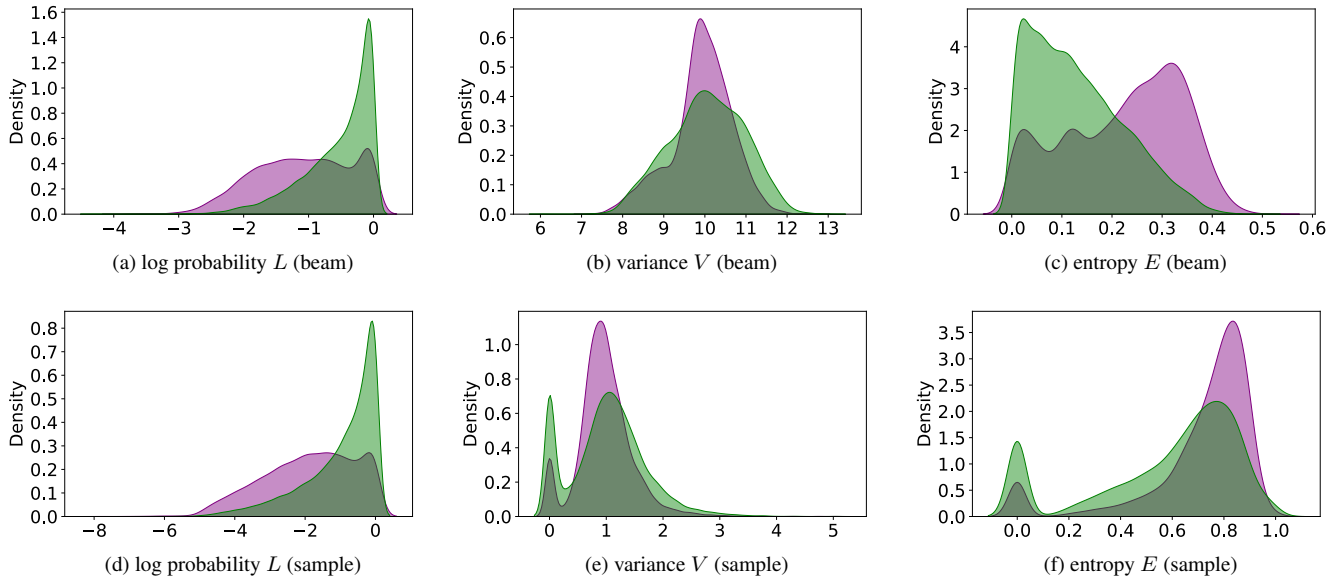


Figure 2. **Probability Metrics.** Visualization of the probability metrics log probability L (Eq. (6)), variance V (Eq. (9)) and entropy E (Eq. (10)) for `true` and `hallucinated` objects. (beam) and (sample) reflect the beam search and nucleus sampling algorithm, respectively.

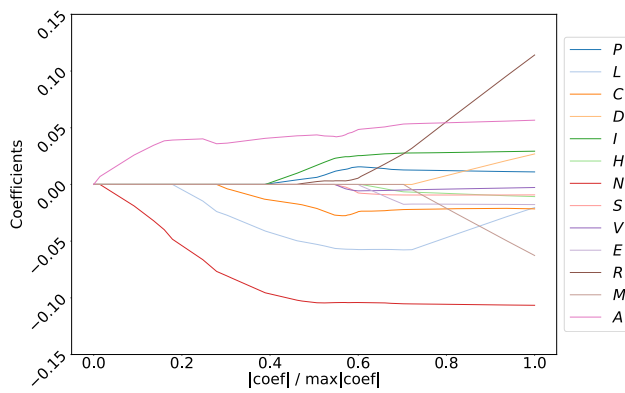


Figure 3. **LASSO Path.** LASSO path for mPLUG-Owl based on nucleus sampling [22] considering the metrics set \mathcal{M} (Eq. (15)). A denotes the maximum of the absolute values of all G weight coefficients for the attention metrics A^g , $g = 0, \dots, G-1$ (Eq. (5)).

pendently from the underlying LVLM or generation method (see Fig. 5 in Appendix B). Tab. 7 lists the average rank of all metrics contained in the metric set \mathcal{M} (Eq. (15)) during the LASSO selection. While most of the metrics are selected during the LASSO path indicated through non-zero coefficients (see Fig. 5), Fig. 4 shows that five metrics are usually enough to achieve high *AUPRC* values. Further metrics only add minor additional information to the classifier. Moreover, we provide the LASSO path including the CLIPScore (Eq. (14)) for mPLUG-Owl [67] and LLaVa

Table 7. **Metric Rank.** The average rank of the metrics \mathcal{M} in the LASSO paths [12, 58] of four state-of-the art LVLMs.

avg. rank	metric	metric name
1.50	N	absolute occurrence (Eq. (4))
2.00	A	mean absolute attention (Eq. (5))
3.00	L	log probability (Eq. (6))
4.00	C	cumulated log probability (Eq. (7))
5.00	I	MSCOCO class index (Eq. (1))
6.50	R	variation ratio (Eq. (11))
8.00	V	variance (Eq. (9))
8.50	H	co-occurrence score (Eq. (2))
8.75	E	entropy (Eq. (10))
9.25	S	score (Eq. (8))
10.25	P	relative position (Eq. (3))
11.50	M	probability margin (Eq. (12))
12.75	D	probability difference (Eq. (13))

[23] in Appendix B. While for mPLUG-Owl, the CLIP-Score is selected first, our proposed absolute occurrence N (Eq. (4)) is the first metric selected in the LLaVa path underlining the informative content induced by our metric.

Finally, we refer to Appendix C to emphasise the importance of our statistical analysis based on the LASSO algorithm. While the relative position P (Eq. (3)) and the probability margin M (Eq. (12)) might look like a proper metric to classify between hallucinated and true objects (see

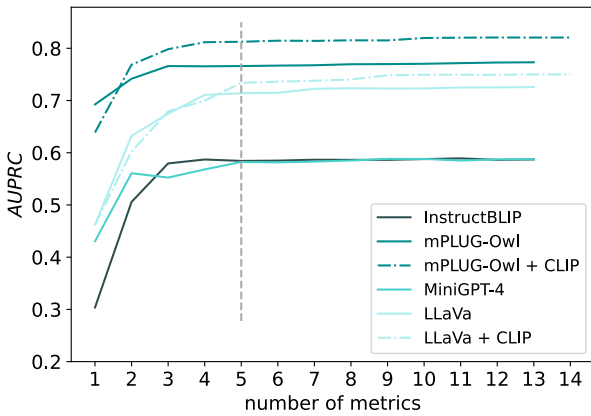


Figure 4. **AUPRC as a Function of the Number of Metrics.** The classification performance of MetaToken in terms of *AUPRC* as a function of the number of metrics for different LVLMs. The metrics are selected along the LASSO path of the respective LVLM.

Table 8. **Integration of MetaToken into LURE.** Results of MetaToken (Ours) plugged into the LURE mitigation method [72]. The superscripts denote the hallucination recall values for the respective method. PR and FPR denote the hallucination precision and false positive rate, respectively. The best results are highlighted, the second best results are underlined.

Method	CHAIR _i ↓	CHAIR _s ↓	PR ↑	FPR ↓
InstructBLIP	LURE ^{76.5}	10.9	29.4	17.5 42.2
	Ours ⁷⁰	9.8	28.2	46.5 9.4
	Ours ⁸⁰	<u>10.3</u>	<u>28.5</u>	<u>37.0</u> <u>15.9</u>
	Ours ⁹⁰	10.6	30.3	26.3 29.5
	Ours ¹⁰⁰	11.6	29.4	10.5 100
mPLUG-Owl	LURE ^{78.6}	14.2	37.1	42.4 46.4
	Ours ⁷⁰	14.4	36.3	71.9 11.9
	Ours ⁸⁰	13.1	33.5	<u>64.8</u> <u>18.8</u>
	Ours ⁹⁰	<u>12.2</u>	<u>31.1</u>	55.1 31.6
	Ours ¹⁰⁰	12.1	30.2	30.3 100

Fig. 7), our analysis shows that these metrics only add minor information to the classifier reflected by an average rank of 10.25 and 11.50, respectively (see Tab. 7).

5.4. MetaToken and Revision of Image Descriptions

In this section, we investigate MetaToken as a substitute for the LURE detection for InstructBLIP [8] and mPLUG-Owl [67]. LURE [72] serves as a hallucination mitigation method using a MiniGPT-4-based revisor to rectify image captions. To this end, LURE applies thresholds on the log probability L (Eq. (6)) and the relative position P (Eq. (3)) to detect possible object hallucinations and replace them

by the *I-don't-know* string "[IDK]". The resulting image caption and the input image are fed into the revisor afterwards to rectify the detected tokens. In our experiments, we replace the threshold-based LURE detection with our proposed MetaToken method (see Sec. 3). Since LURE evaluates all objects instead of being restricted to the MSCOCO dataset [37], we train our classifier on the general set of metrics

$$\mathcal{M}^* = \{P_{o_j}, N_{o_j}, A_{o_j}^0, \dots, A_{o_j}^{G-1}, L_{o_j}, C_{o_j}, S_{o_j}, V_{o_j}, E_{o_j}, R_{o_j}, M_{o_j}, D_{o_j}\} \quad (23)$$

abstaining from the MSCOCO-related metrics I (Eq. (1)) and H (Eq. (2)). The results are stated in Appendix D. In accordance with Fig. 4, we observe almost no performance drop when considering the general metric set \mathcal{M}^* .

First of all note that as in [70], we are not able to reproduce the results in [72] with respect to InstructBLIP. While we achieve a hallucination rate of 10.4% for InstructBLIP captions (see Tab. 3), the rectified image captions by LURE include 10.9% of hallucinations, even increasing the amount of hallucinated objects (see Tab. 8). We believe that this observation results from the fact that MiniGPT-4 has a higher hallucination rate than InstructBLIP (see Tab. 3). Since the LURE detection has a false positive rate (FPR) of 42.2%, as stated in Tab. 8, we guess that the MiniGPT-4-based revisor replaces true objects by hallucinated objects, even though the revisor is fine-tuned to mitigate hallucinations.

However, using our detection method, we are able to mitigate hallucinations achieving CHAIR_i values of 9.8%. To this end, note that we can control the precision-recall-ratio in our method by varying the decision threshold of our lightweight meta classifier. For a recall of 70%, we observe a FPR of 9.4% only. Thus, we prevent the revisor from including additional hallucinations by replacing false positives, that is, true objects. The results in Tab. 8 confirm our assumption on InstructBLIP: The higher the FPR, the higher the number of hallucinations induced by the revisor.

On the other hand, LURE reduced the number of hallucinations for mPLUG-Owl by 52.98%, i.e. from 30.2% to 14.2% with a FPR of 46.4%. Since the revisor induces substantially less hallucinations than mPLUG-Owl, the correction of true positives outweighs the potential introduction of new hallucinations by replacing false positives. In fact, we observe from Tab. 8 that higher recall values, and thus, higher FPRs, lead to consistently lower hallucination rates for mPLUG-Owl. However, note that the superior precision-recall-ratio from our approach also outperforms the LURE results on mPLUG-Owl: For a recall of 80% (which is closest to the LURE detection of 78.6%), we reduce the proportion of hallucinations by 56.62% to 13.1%, that is, 3.64% less hallucinations compared to the LURE baseline.

6. Limitations

While MetaToken achieves high classification performance, it still has room for improvement for strong LVLMs inducing only few hallucinations. For these models, a high hallucination recall rate can be achieved at the cost of a high false positive rate. Moreover, our method is restricted to the problem of object instance hallucination detection in image captions, while the detection of attribute-level hallucinations still remains an unsolved problem we will tackle in future work. Lastly, our method is based on the hand-crafted CHAIR method [52] based on human annotations. While this evaluation method relies on exact matching, it still leads to mismatches due to misinterpretations of the generated language output of LVLMs.

7. Conclusion

In this paper, we introduce MetaToken, a novel lightweight hallucination detection technique for LVLMs based on meta classification. Inspired by recently discovered causes of hallucinations, we propose and analyse a broad set of potential factors for hallucinations in LVLMs. Based on a comprehensive statistical analysis of these factors, we reveal key indicators of hallucinations which have been overseen in previous works. We evaluate our method on four state-of-the-art LVLMs and different generation configurations achieving *AUROC* values of up to 92.19% and *AUPRC* values of up to 82.69%. Moreover, we show that our lightweight classifier reliably detects hallucinations inducing an *ECE* between 0.81% and 2.01%. Finally, we demonstrate that MetaToken can be easily integrated into the LURE mitigation method reducing the hallucination rate by up to 56.62%, i.e., 3.64% less hallucinations than the LURE baseline. As future work, we will tackle the problem of attribute-level hallucination detection for general visual question answering tasks.

Disclaimer

The results, opinions and conclusions expressed in this publication are not necessarily those of Volkswagen Aktiengesellschaft.

References

- [1] Jean-Baptiste Alayrac, Jeff Donahue, Pauline Luc, Antoine Miech, Iain Barr, Yana Hasson, Karel Lenc, Arthur Mensch, Katherine Millican, Malcolm Reynolds, Roman Ring, Eliza Rutherford, Serkan Cabi, Tengda Han, Zhitao Gong, Sina Samangooei, Marianne Monteiro, Jacob L. Menick, Sebastian Borgeaud, Andy Brock, Aida Nematzadeh, Sahand Sharifzadeh, Mikołaj Bińkowski, Ricardo Barreira, Oriol Vinyals, Andrew Zisserman, and Karén Simonyan. Flamingo: A visual language model for few-shot learning. In *Advances in Neural Information Processing Systems*, pages 23716–23736. Curran Associates, Inc, 2022.
- [2] Peter Anderson, Basura Fernando, Mark Johnson, and Stephen Gould. Spice: Semantic propositional image caption evaluation. In *Computer Vision – ECCV 2016*, pages 382–398, Cham, 2016. Springer International Publishing.
- [3] R. Bisiani. Beam search. *Encyclopedia of Artificial Intelligence*, pages 56–58, 1987.
- [4] Tom B. Brown, Benjamin Mann, Nick Ryder, Melanie Subbiah, Jared Kaplan, Prafulla Dhariwal, Arvind Neelakantan, Pranav Shyam, Girish Sastry, Amanda Askell, Sandhini Agarwal, Ariel Herbert-Voss, Gretchen Krueger, Tom Henighan, Rewon Child, Aditya Ramesh, Daniel M. Ziegler, Jeffrey Wu, Clemens Winter, Christopher Hesse, Mark Chen, Eric Sigler, Mateusz Litwin, Scott Gray, Benjamin Chess, Jack Clark, Christopher Berner, Sam McCandlish, Alec Radford, Ilya Sutskever, and Dario Amodei. Language models are few-shot learners. In *Proceedings of the 34th International Conference on Neural Information Processing Systems*, Red Hook, NY, USA, 2020. Curran Associates Inc.
- [5] Tongfei Chen, Jiri Navratil, Vijay Iyengar, and Karthikeyan Shanmugam. Confidence scoring using whitebox meta-models with linear classifier probes. In *Proceedings of the Twenty-Second International Conference on Artificial Intelligence and Statistics*, pages 1467–1475. PMLR, 2019.
- [6] Xiang Chen, Chenxi Wang, Yida Xue, Ningyu Zhang, Xiaoyan Yang, Qian Li, Yue Shen, Lei Liang, Jinjie Gu, and Huajun Chen. Unified hallucination detection for multimodal large language models. *ArXiv*, abs/2402.03190, 2024.
- [7] Aakanksha Chowdhery, Sharan Narang, Jacob Devlin, Maarten Bosma, Gaurav Mishra, Adam Roberts, Paul Barham, Hyung Won Chung, Charles Sutton, Sebastian Gehrmann, Parker Schuh, Kensen Shi, Sasha Tsvyashchenko, Joshua Maynez, Abhishek Rao, Parker Barnes, Yi Tay, Noam Shazeer, Vinodkumar Prabhakaran, Emily Reif, Du Nan, Ben Hutchinson, Reiner Pope, James Bradbury, Jacob Austin, Michael Isard, Guy Gur-Ari, Pengcheng Yin, Toju Duke, Anselm Levskaya, Sanjay Ghemawat, Sunipa Dev, Henryk Michalewski, Xavier Garcia, Vedant Misra, Kevin Robinson, Liam Fedus, Denny Zhou, Daphne Ippolito, David Luan, Hyeontaek Lim, Barret Zoph, Alexander Spiridonov, Ryan Sepassi, David Dohan, Shivani Agrawal, Mark Omernick, Andrew M. Dai, Thanumalayan Sankaranarayana Pillai, Marie Pellat, Aitor Lewkowycz, Erica Moreira, Rewon Child, Oleksandr Polozov, Katherine Lee, Zongwei Zhou, Xuezhi Wang, Brennan Saeta, Mark Diaz, Orhan Firat, Michele Catasta, Jason Wei, Kathy Meier-Hellstern, Douglas Eck, Jeff Dean, Slav Petrov, and Noah Fiedel. Palm: Scaling language modeling with pathways. *Journal of Machine Learning Research*, 24(240):1–113, 2023.
- [8] Wenliang Dai, Junnan Li, DONGXU LI, Anthony Tiong, Junqi Zhao, Weisheng Wang, Boyang Li, Pascale N. Fung, and Steven Hoi. Instructblip: Towards general-purpose vision-language models with instruction tuning. In *Advances in Neural Information Processing Systems*, pages 49250–49267. Curran Associates, Inc, 2023.

[9] Wenliang Dai, Zihan Liu, Ziwei Ji, Dan Su, and Pascale Fung. Plausible may not be faithful: Probing object hallucination in vision-language pre-training. In *Proceedings of the 17th Conference of the European Chapter of the Association for Computational Linguistics*, pages 2136–2148, Dubrovnik, Croatia, 2023. Association for Computational Linguistics.

[10] Jesse Davis and Mark Goadrich. The relationship between precision-recall and roc curves. In *Proceedings of the 23rd International Conference on Machine Learning*, pages 233–240, New York, NY, USA, 2006. Association for Computing Machinery.

[11] Yifan Du, Zikang Liu, Junyi Li, and Wayne Xin Zhao. A survey of vision-language pre-trained models. In *Proceedings of the Thirty-First International Joint Conference on Artificial Intelligence, IJCAI-22*, pages 5436–5443. International Joint Conferences on Artificial Intelligence Organization, 2022.

[12] Bradley Efron, Trevor Hastie, Iain Johnstone, and Robert Tibshirani. Least angle regression. *The Annals of Statistics*, 32(2):407–499, 2004.

[13] Laura Fieback, Bidya Dash, Jakob Spiegelberg, and Hanno Gottschalk. Temporal performance prediction for deep convolutional long short-term memory networks. In *Advanced Analytics and Learning on Temporal Data*, pages 145–158, Cham, 2023. Springer Nature Switzerland.

[14] Chaoyou Fu, Peixian Chen, Yunhang Shen, Yulei Qin, Mengdan Zhang, Xu Lin, Zhenyu Qiu, Wei Lin, Jinrui Yang, Xiawu Zheng, Ke Li, Xing Sun, and Rongrong Ji. Mme: A comprehensive evaluation benchmark for multimodal large language models. *ArXiv*, abs/2306.13394, 2023.

[15] Fuxiao Liu and Kevin Lin and Linjie Li and Jianfeng Wang and Yaser Yacoob and Lijuan Wang. Mitigating hallucination in large multi-modal models via robust instruction tuning. *ArXiv*, abs/2306.14565, 2023.

[16] Haoxiang Gao, Yaqian Li, Kaiwen Long, Ming Yang, and Yiqing Shen. A survey for foundation models in autonomous driving. *ArXiv*, abs/2402.01105, 2024.

[17] Tao Gong, Chengqi Lyu, Shilong Zhang, Yudong Wang, Miao Zheng, Qianmengke Zhao, Kuikun Liu, Wenwei Zhang, Ping Luo, and Kai Chen. Multimodal-gpt: A vision and language model for dialogue with humans. *ArXiv*, abs/2305.04790, 2023.

[18] Yu Gui, Ying Jin, and Zhimei Ren. Conformal alignment: Knowing when to trust foundation models with guarantees. *ArXiv*, 2024.

[19] Anish Gunjal, Jihan Yin, and Erhan Bas. Detecting and preventing hallucinations in large vision language models. *ArXiv*, abs/2308.06394, 2023.

[20] Dan Hendrycks and Kevin Gimpel. A baseline for detecting misclassified and out-of-distribution examples in neural networks. In *Proceedings of International Conference on Learning Representations*, 2017.

[21] Jack Hessel, Ari Holtzman, Maxwell Forbes, Ronan Le Bras, and Yejin Choi. Clipscore: A reference-free evaluation metric for image captioning. In *Proceedings of the 2021 Conference on Empirical Methods in Natural Language Processing*, pages 7514–7528, Online and Punta Cana, Dominican Republic, 2021. Association for Computational Linguistics.

[22] Ari Holtzman, Jan Buys, Du Li, Maxwell Forbes, and Yejin Choi. The curious case of neural text degeneration. In *8th International Conference on Learning Representations, ICLR 2020, Addis Ababa, Ethiopia, April 26-30, 2020*. OpenReview.net, 2020.

[23] Jiaxing Huang, Jingyi Zhang, Kai Jiang, Han Qiu, and Shijian Lu. Visual instruction tuning towards general-purpose multimodal model: A survey. *ArXiv*, abs/2312.16602, 2023.

[24] Chao Jia, Yinfei Yang, Ye Xia, Yi-Ting Chen, Zarana Parekh, Hieu Pham, Quoc Le, Yun-Hsuan Sung, Zhen Li, and Tom Duerig. Scaling up visual and vision-language representation learning with noisy text supervision. In *Proceedings of the 38th International Conference on Machine Learning*, pages 4904–4916. PMLR, 2021.

[25] Yixing Jiang, Jesutofunmi A. Omiye, Cyril Zakka, Michael Moor, Haiwen Gui, Shayan Alipour, Seyed Shahabeddin Mousavi, Jonathan H. Chen, Pranav Rajpurkar, and Roxana Daneshjou. Evaluating general vision-language models for clinical medicine. *medRxiv*, 2024.

[26] Liqiang Jing, Ruosen Li, Yunmo Chen, Mengzhao Jia, and Du Xinya. Faithscore: Evaluating hallucinations in large vision-language models. *ArXiv*, abs/2311.01477, 2023.

[27] Wonjae Kim, Bokyung Son, and Ildoo Kim. Vilt: Vision-and-language transformer without convolution or region supervision. In *Proceedings of the 38th International Conference on Machine Learning*, pages 5583–5594. PMLR, 2021.

[28] Kamil Kowol, Matthias Rottmann, Stefan Bracke, and Hanno Gottschalk. Yodar: Uncertainty-based sensor fusion for vehicle detection with camera and radar sensors. In *International Conference on Agents and Artificial Intelligence*, 2020.

[29] Alon Lavie and Abhaya Agarwal. Meteor: An automatic metric for mt evaluation with high levels of correlation with human judgments. In *Proceedings of the Second Workshop on Statistical Machine Translation*, pages 228–231, USA, 2007. Association for Computational Linguistics.

[30] Sicong Leng, Hang Zhang, Guanzheng Chen, Xin Li, Shijian Lu, Chunyan Miao, and Li Bing. Mitigating object hallucinations in large vision-language models through visual contrastive decoding. *ArXiv*, abs/2311.16922, 2023.

[31] Chen Li, Yixiao Ge, Dian Li, and Ying Shan. Vision-language instruction tuning: A review and analysis. *ArXiv*, abs/2311.08172, 2023.

[32] Chunyuan Li, Cliff Wong, Sheng Zhang, Naoto Usuyama, Haotian Liu, Jianwei Yang, Tristan Naumann, Hoifung Poon, and Jianfeng Gao. Llava-med: Training a large language-and-vision assistant for biomedicine in one day. In *Advances in Neural Information Processing Systems*, pages 28541–28564. Curran Associates, Inc, 2023.

[33] Junnan Li, Ramprasaath Selvaraju, Akhilesh Gotmare, Shafiq Joty, Caiming Xiong, and Steven Chu Hong Hoi. Align before fuse: Vision and language representation learning with momentum distillation. In *Advances in Neural Information Processing Systems*, pages 9694–9705. Curran Associates, Inc, 2021.

[34] Junnan Li, DONGXU LI, Caiming Xiong, and Steven Hoi. Blip: Bootstrapping language-image pre-training for unified

vision-language understanding and generation. In *Proceedings of the 39th International Conference on Machine Learning*, pages 12888–12900. PMLR, 2022.

[35] Liunian Harold Li, Mark Yatskar, Da Yin, Cho-Jui Hsieh, and Kai-Wei Chang. Visualbert: A simple and performant baseline for vision and language. *ArXiv*, abs/1908.03557, 2019.

[36] Yifan Li, Yifan Du, Kun Zhou, Jinpeng Wang, Xin Zhao, and Ji-Rong Wen. Evaluating object hallucination in large vision-language models. In *Proceedings of the 2023 Conference on Empirical Methods in Natural Language Processing*, pages 292–305, Singapore, 2023. Association for Computational Linguistics.

[37] Tsung-Yi Lin, Michael Maire, Serge Belongie, James Hays, Pietro Perona, Deva Ramanan, Piotr Dollár, and C. Lawrence Zitnick. Microsoft coco: Common objects in context. In *Computer Vision – ECCV 2014*, pages 740–755, Cham, 2014. Springer International Publishing.

[38] Wei-Hao Lin and Alexander Hauptmann. Metaclassification: Combining multimodal classifiers. In *Mining Multimedia and Complex Data*, pages 217–231, Berlin, Heidelberg, 2003. Springer Berlin Heidelberg.

[39] Fuxiao Liu, Tianrui Guan, Xiyang Wu, Zongxia Li, Lichang Chen, Yaser Yacoob, Dinesh Manocha, and Tianyi Zhou. Hallusionbench: You see what you think? or you think what you see? an image-context reasoning benchmark challenging for gpt-4v(ision), llava-1.5, and other multi-modality models. *ArXiv*, abs/2310.14566, 2023.

[40] Hanchao Liu, Wenyuan Xue, Yifei Chen, Dapeng Chen, Xiutian Zhao, Ke Wang, Liping Hou, Rong-Zhi Li, and Wei Peng. A survey on hallucination in large vision-language models. *ArXiv*, abs/2402.00253, 2024.

[41] Tianyu Liu, Yizhe Zhang, Chris Brockett, Yi Mao, Zhifang Sui, Weizhu Chen, and Bill Dolan. A token-level reference-free hallucination detection benchmark for free-form text generation. In *Proceedings of the 60th Annual Meeting of the Association for Computational Linguistics (Volume 1: Long Papers)*, pages 6723–6737, Dublin, Ireland, 2022. Association for Computational Linguistics.

[42] Yuanzhan Liu, Haodong Duan, Yuanhan Zhang, Bo Li, Songyang Zhang, Wangbo Zhao, Yike Yuan, Jiaqi Wang, Conghui He, Ziwei Liu, Kai Chen, and Dahua Lin. Mmbench: Is your multi-modal model an all-around player? *ArXiv*, abs/2307.06281, 2023.

[43] Holy Lovenia, Wenliang Dai, Samuel Cahyawijaya, Ziwei Ji, and Pascale Fung. Negative object presence evaluation (nope) to measure object hallucination in vision-language models. *ArXiv*, abs/2310.05338, 2023.

[44] Jiasen Lu, Jianwei Yang, Dhruv Batra, and Devi Parikh. Neural baby talk. In *2018 IEEE/CVF Conference on Computer Vision and Pattern Recognition*, pages 7219–7228, 2018.

[45] Kira Maag, Matthias Rottmann, and Hanno Gottschalk. Time-dynamic estimates of the reliability of deep semantic segmentation networks. In *2020 IEEE 32nd International Conference on Tools with Artificial Intelligence (ICTAI)*, pages 502–509, 2020.

[46] Kira Maag, Matthias Rottmann, Serin Varghese, Fabian Hüger, Peter Schlücht, and Hanno Gottschalk. Improving video instance segmentation by light-weight temporal uncertainty estimates. In *2021 International Joint Conference on Neural Networks (IJCNN)*, pages 1–8, 2021.

[47] Potsawee Manakul, Adian Liusie, and Mark Gales. Self-checkgpt: Zero-resource black-box hallucination detection for generative large language models. In *Proceedings of the 2023 Conference on Empirical Methods in Natural Language Processing*, pages 9004–9017, Singapore, 2023. Association for Computational Linguistics.

[48] Mahdi Pakdaman Naeini, Gregory Cooper, and Milos Hauskrecht. Obtaining well calibrated probabilities using bayesian binning. *Proceedings of the AAAI Conference on Artificial Intelligence*, 29(1), 2015.

[49] Kishore Papineni, Salim Roukos, Todd Ward, and Wei-Jing Zhu. Bleu: A method for automatic evaluation of machine translation. In *Proceedings of the 40th Annual Meeting of the Association for Computational Linguistics*, pages 311–318, Philadelphia, Pennsylvania, USA, 2002. Association for Computational Linguistics.

[50] Alec Radford, Jong Wook Kim, Chris Hallacy, Aditya Ramesh, Gabriel Goh, Sandhini Agarwal, Girish Sastry, Amanda Askell, Pamela Mishkin, Jack Clark, Gretchen Krueger, and Ilya Sutskever. Learning transferable visual models from natural language supervision. In *Proceedings of the 38th International Conference on Machine Learning*, pages 8748–8763. PMLR, 2021.

[51] Colin Raffel, Noam Shazeer, Adam Roberts, Katherine Lee, Sharan Narang, Michael Matena, Yanqi Zhou, Wei Li, and Peter J. Liu. Exploring the limits of transfer learning with a unified text-to-text transformer. *Journal of Machine Learning Research*, 21(140):1–67, 2020.

[52] Anna Rohrbach, Lisa Anne Hendricks, Kaylee Burns, Trevor Darrell, and Kate Saenko. Object hallucination in image captioning. In *Proceedings of the 2018 Conference on Empirical Methods in Natural Language Processing*, pages 4035–4045, Brussels, Belgium, 2018. Association for Computational Linguistics.

[53] Matthias Rottmann and Marius Schubert. Uncertainty measures and prediction quality rating for the semantic segmentation of nested multi resolution street scene images. In *2019 IEEE/CVF Conference on Computer Vision and Pattern Recognition Workshops (CVPRW)*, pages 1361–1369, 2019.

[54] Matthias Rottmann, Pascal Colling, Thomas Paul Hack, Robin Chan, Fabian Hüger, Peter Schlücht, and Hanno Gottschalk. Prediction error meta classification in semantic segmentation: Detection via aggregated dispersion measures of softmax probabilities. In *2020 International Joint Conference on Neural Networks (IJCNN)*, pages 1–9, 2020.

[55] Marius Schubert, Karsten Kahl, and Matthias Rottmann. Metadetect: Uncertainty quantification and prediction quality estimates for object detection. In *2021 International Joint Conference on Neural Networks (IJCNN)*, pages 1–10, 2021.

[56] C. E. Shannon. A mathematical theory of communication. *The Bell System Technical Journal*, 27(3):379–423, 1948.

[57] Xiaoyu Tian, Junru Gu, Bailin Li, Yicheng Liu, Chenxu Hu, Yang Wang, Kun Zhan, Peng Jia, Xianpeng Lang, and Hang Zhao. Drivevlm: The convergence of autonomous driving and large vision-language models. *ArXiv*, abs/2402.12289, 2024.

[58] Robert Tibshirani. Regression shrinkage and selection via the lasso. *Journal of the Royal Statistical Society: Series B (Methodological)*, 58(1):267–288, 2018.

[59] Hugo Touvron, Thibaut Lavril, Gautier Izacard, Xavier Martinet, Marie-Anne Lachaux, Timothée Lacroix, Baptiste Rozière, Naman Goyal, Eric Hambro, Faisal Azhar, Aurelien Rodriguez, Armand Joulin, Edouard Grave, and Guillaume Lample. Llama: Open and efficient foundation language models. *ArXiv*, abs/2302.13971, 2023.

[60] Vishal Thanvantri Vasudevan, Abhinav Sethy, and Alireza Roshan Ghias. Towards better confidence estimation for neural models. In *ICASSP 2019 - 2019 IEEE International Conference on Acoustics, Speech and Signal Processing (ICASSP)*, pages 7335–7339, 2019.

[61] Ramakrishna Vedantam, C. Lawrence Zitnick, and Devi Parikh. Cider: Consensus-based image description evaluation. In *2015 IEEE Conference on Computer Vision and Pattern Recognition (CVPR)*, pages 4566–4575, 2015.

[62] Junyan Wang, Yi Zhou, Guohai Xu, Pengcheng Shi, Chenlin Zhao, Haiyang Xu, Qinghao Ye, Mingshi Yan, Ji Zhang, Jihua Zhu, Jitao Sang, and Haoyu Tang. Evaluation and analysis of hallucination in large vision-language models. *ArXiv*, abs/2308.15126, 2023.

[63] Lei Wang, Jiabang He, Shenshen Li, Ning Liu, and Ee-Peng Lim. Mitigating fine-grained hallucination by fine-tuning large vision-language models with caption rewrites. In *MultiMedia Modeling*, pages 32–45, Cham, 2024. Springer Nature Switzerland.

[64] Peng Wang, An Yang, Rui Men, Junyang Lin, Shuai Bai, Zhikang Li, Jianxin Ma, Chang Zhou, Jingren Zhou, and Hongxia Yang. Ofa: Unifying architectures, tasks, and modalities through a simple sequence-to-sequence learning framework. In *Proceedings of the 39th International Conference on Machine Learning*, pages 23318–23340. PMLR, 2022.

[65] Jun Wu, Q. Liu, Ding Wang, Jinghao Zhang, Shu Wu, Liang Wang, and Tien-Ping Tan. Logical closed loop: Uncovering object hallucinations in large vision-language models. *ArXiv*, abs/2402.11622, 2024.

[66] Shangyu Xing, Fei Zhao, Zhen Wu, Tuo An, Weihao Chen, Chunhui Li, Jianbing Zhang, and Xinyu Dai. Efuf: Efficient fine-grained unlearning framework for mitigating hallucinations in multimodal large language models. *ArXiv*, abs/2402.09801, 2024.

[67] Qinghao Ye, Haiyang Xu, Guohai Xu, Jiabo Ye, Ming Yan, Yi Zhou, Junyan Wang, Anwen Hu, Pengcheng Shi, Yaya Shi, Chenliang Li, Yuanhong Xu, Hehong Chen, Junfeng Tian, Qiang Qi, Ji Zhang, and Feiyan Huang. mplug-owl: Modularization empowers large language models with multimodality. *ArXiv*, abs/2304.14178, 2023.

[68] Shukang Yin, Chaoyou Fu, Sirui Zhao, Tong Xu, Hao Wang, Dianbo Sui, Yunhang Shen, Ke Li, Xingguo Sun, and Enhong Chen. Woodpecker: Hallucination correction for multimodal large language models. *ArXiv*, abs/2310.16045, 2023.

[69] Weihao Yu, Zhengyuan Yang, Linjie Li, Jianfeng Wang, Kevin Lin, Zicheng Liu, Xinchao Wang, and Lijuan Wang. Mm-vet: Evaluating large multimodal models for integrated capabilities. *ArXiv*, abs/2308.02490, 2023.

[70] Linxi Zhao, Yihe Deng, Weitong Zhang, and Quanquan Gu. Mitigating object hallucination in large vision-language models via classifier-free guidance. *ArXiv*, abs/2402.08680, 2024.

[71] Wayne Xin Zhao, Kun Zhou, Junyi Li, Tianyi Tang, Xiaolei Wang, Yupeng Hou, Yingqian Min, Beichen Zhang, Junjie Zhang, Zican Dong, Du Yifan, Chen Yang, Yushuo Chen, Z. Chen, Jinhao Jiang, Ruiyang Ren, Yifan Li, Xinyu Tang, Zikang Liu, Peiyu Liu, Jianyun Nie, and Ji-Rong Wen. A survey of large language models. *ArXiv*, abs/2303.18223, 2023.

[72] Yiyang Zhou, Chenhang Cui, Jaehong Yoon, Linjun Zhang, Zhun Deng, Chelsea Finn, Mohit Bansal, and Huaxiu Yao. Analyzing and mitigating object hallucination in large vision-language models. *ArXiv*, abs/2310.00754, 2023.

[73] Deyao Zhu, Jun Chen, Xiaoqian Shen, Xiang Li, and Mohamed Elhoseiny. Minigpt-4: Enhancing vision-language understanding with advanced large language models. *ArXiv*, abs/2304.10592, 2023.

MetaToken: Detecting Hallucination in Image Descriptions by Meta Classification

Supplementary Material

A. Meta Classifier Configurations

In our experiments, we use the `sklearn.linear_model.LogisticRegression`² and `sklearn.ensemble.GradientBoostingClassifier`³ methods with scikit-learn version 1.3.2. Tab. 9 states the applied configurations. For those parameters not listed in Tab. 9, we refer to the default settings.

B. LASSO Path

We analyze the informative content included in the metrics proposed in Sec. 3.2 for the considered LVLMs InstructBLIP (Vicuna-7B) [8], mPLUG-Owl (LLaMA-7B) [67], MiniGPT-4 (Vicuna-7B) [73], and LLaVa 1.5 (Vicuna-7B) [23] based on nucleus sampling [22]. For InstructBLIP and mPLUG-Owl we further investigated the considered metrics based on beam search [3]. To this end, we make use of the least absolute shrinkage and selection operator (LASSO) algorithm [12, 58] to analyze the predictive power of the metrics considered. The LASSO method performs a variable selection for a linear regression including the estimation of the corresponding coefficients ranking the most informative metrics. Fig. 5 shows the LASSO paths for the considered LVLMs and generation configurations. While the metrics absolute occurrence N (Eq. (4)), mean absolute attention A (Eq. (5)), log probability L (Eq. (6)) and cumulated log probability C (Eq. (7)) are selected first in almost all settings, we observe different metric ranks between the sampling-based captions and beam search-based captions. While the coefficient for the entropy E (Eq. (10)) is vanishing for the sampled captions (see Figs. 5a, 5b, 5e and 5f), it is selected as the sixth metric for the beam search-based captions (see Figs. 5c and 5d).

Moreover, we investigate the LASSO paths for the extended metric set $\mathcal{M}^{\text{clip}}$ (Eq. (16)) for the LVLMs sharing the vision encoder with CLIP [50], that is, mPLUG-Owl and LLaVa in Fig. 6. For mPLUG-Owl, the *CLIP* metric (Eq. (14)) is selected as the first metric as we can see in Fig. 6a followed by the mean absolute attention A (Eq. (5)) the absolute occurrence N (Eq. (4)) and the log probability L (Eq. (6)). For LLaVa, on the other hand, our proposed metric absolute occurrence N (Eq. (4)) is selected first, followed by the *CLIP* metric (Eq. (14)), the log probability L

²https://scikit-learn.org/1.3/modules/generated/sklearn.linear_model.LogisticRegression.html

³<https://scikit-learn.org/1.3/modules/generated/sklearn.ensemble.GradientBoostingClassifier.html>

Table 9. Classifier Configurations. The configurations applied in our experiments for the `sklearn.linear_model.LogisticRegression` (LR) and `sklearn.ensemble.GradientBoostingClassifier` (GB) classifier.

	LR	GB
scikit-learn	1.3.2	1.3.2
random_state	0	0
solver	saga	-
max_iter	1000	-
tol	1e-3	-

(Eq. (6)) and cumulated log probability C (Eq. (7)).

C. Metric Visualization

In order to provide a visual analysis of our proposed metrics (see Sec. 3.2), we plot our metrics for true and hallucinated objects in Figs. 7 and 8. While some of the attention metrics $A^g, g = 0, \dots, 31$ fully overlap for true and hallucinated objects (see Fig. 8), for specific attention heads like $g = 9, 24$ and 28 the respective metrics distinguish between hallucinated and true objects. We can also see in Fig. 7 that our proposed metric absolute occurrence N (Eq. (4)) has a high density for $N = 1$ for hallucinated objects, that is, if the object is only mentioned once in the image caption. True objects usually occur several times in the image caption. However, we want to emphasise the importance of our statistical analysis based on the LASSO algorithm in Appendix B. While in Fig. 7, the relative position P (Eq. (3)) might look like a better metric to classify between hallucinated and true objects than the log probability L (Eq. (6)) or the cumulated log probability C (Eq. (7)), our analysis in the previous section shows that the relative position P only add minor information to the classifier reflected by a rather small coefficient compared to the log probability L and cumulated log probability C (see Fig. 5).

D. Metric Combination

Since recent works [36, 72] have shown that LVLMs are prone to hallucinate (co-occurring) MSCOCO objects [37], we include the MSCOCO class index I (Eq. (1)) and the co-occurrence score H (Eq. (2)) into our proposed set of metrics \mathcal{M} . However, in order to provide a general method, which can be applied to any dataset without any restrictions, we investigate the performance of MetaToken with respect

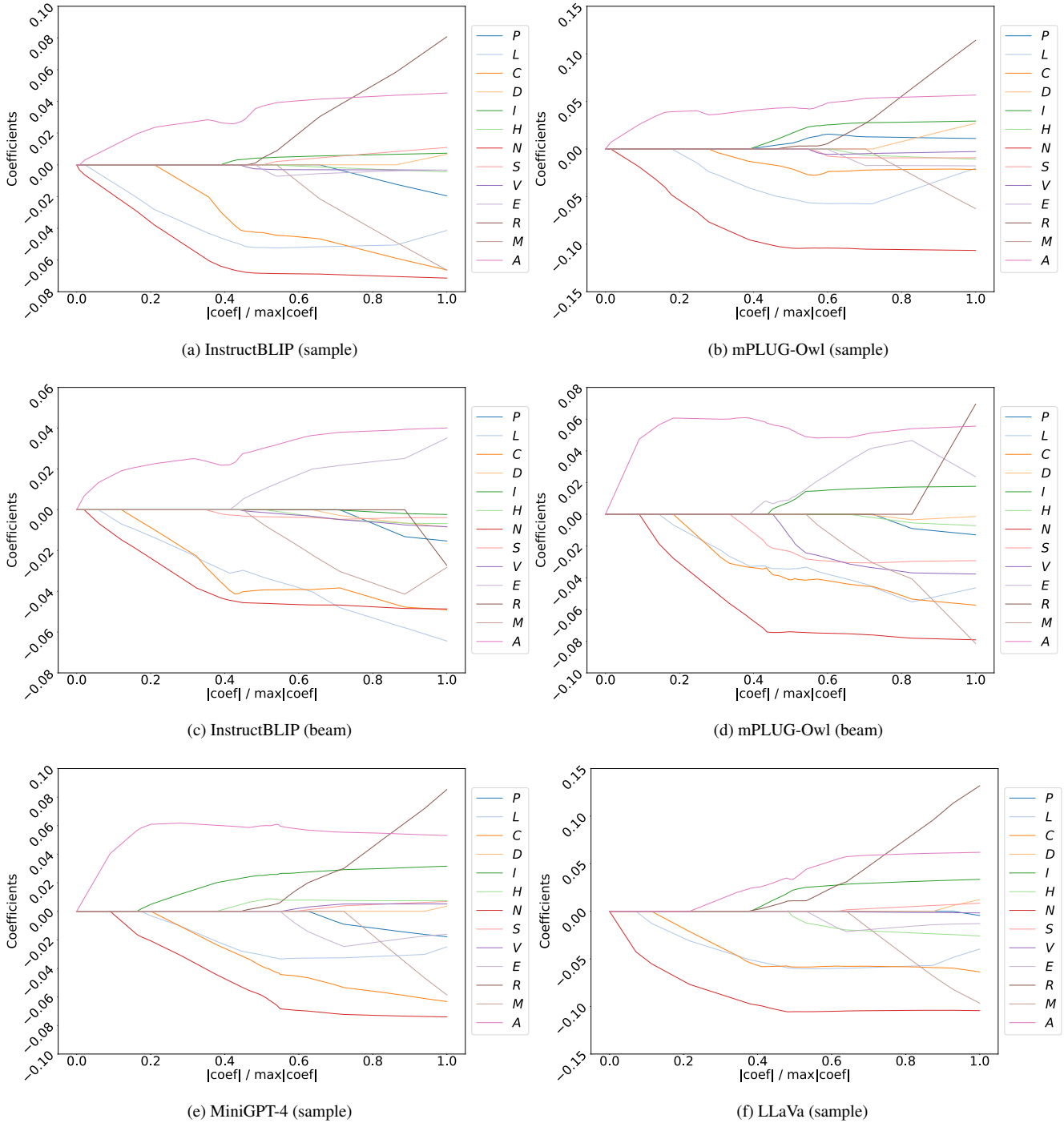


Figure 5. **LASSO path.** LASSO path for the set of metrics \mathcal{M} (Eq. (15)). A denotes the maximum of the absolute values of all G weight coefficients for the attention metrics $A^g, g = 0, \dots, G - 1$ (Eq. (5)). (beam) and (sample) reflect the beam search and nucleus sampling algorithm, respectively.

to the general set of metrics \mathcal{M}^* (Eq. (23)) abstaining from the MSCOCO-related metrics I and H . The results are provided in Tab. 10. Even though our exploration from Ap-

pendix B shows that the MSCOCO class index I is usually under the top five metrics selected, we observe almost no performance drop in the classification results for \mathcal{M}^* .

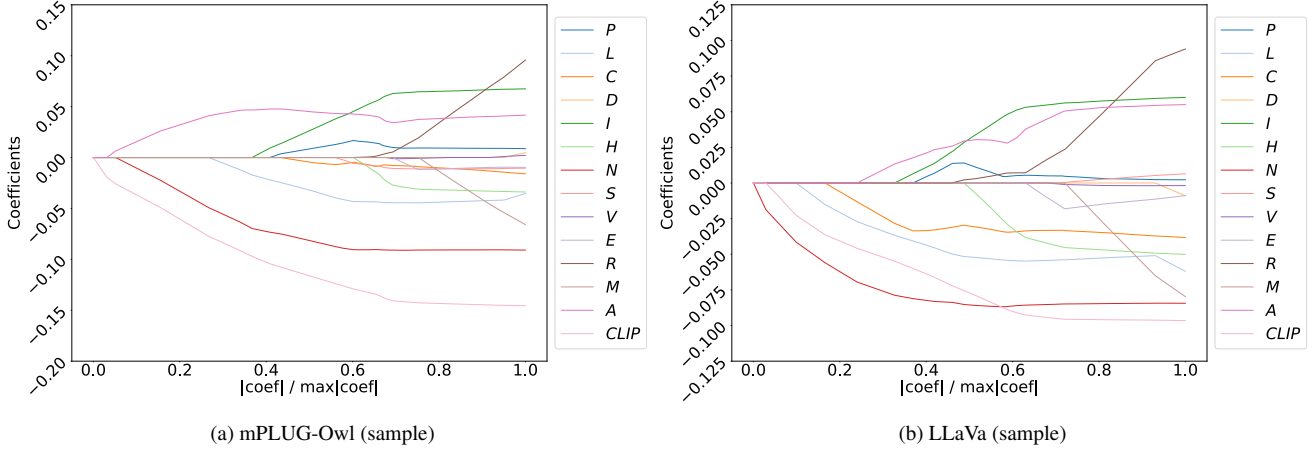


Figure 6. **LASSO path.** LASSO path for the set of metrics $\mathcal{M}^{\text{clip}}$ (Eq. (16)). A denotes the maximum of the absolute values of all G weight coefficients for the attention metrics $A^g, g = 0, \dots, G - 1$ (Eq. (5)). (beam) and (sample) reflect the beam search and nucleus sampling algorithm, respectively.

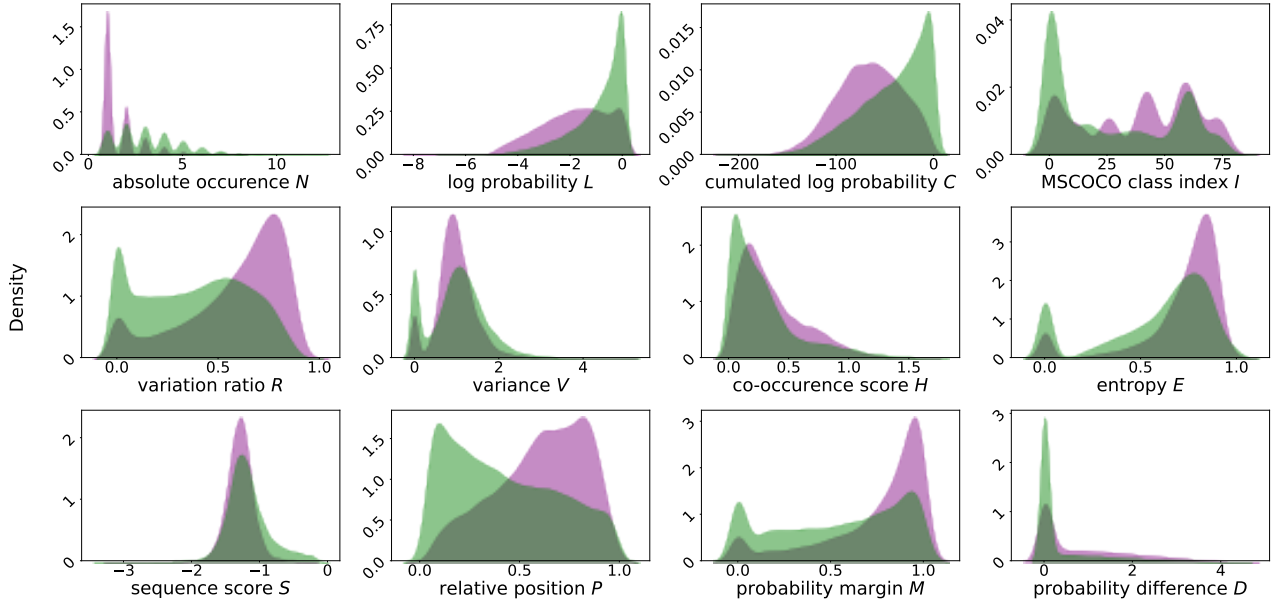


Figure 7. **Metrics.** Visualization of a selection of our proposed input metrics defined in Sec. 3.2 for `true` and `hallucinated` objects.

Table 10. **Experimental Results for different Set of Metrics.** Hallucination detection results for InstructBLIP [8] and mPLUG-Owl [67] for the MSCOCO [37] specific metric set \mathcal{M} (Eq. (15)) and the general set \mathcal{M}^* (Eq. (23)). The classifier based on logistic regression and gradient boosting are denoted by LR and GB, respectively. The best results are highlighted.

	ACC (in %) \uparrow		$AUROC$ (in %) \uparrow		$AUPRC$ (in %) \uparrow	
	LR	GB	LR	GB	LR	GB
InstructBLIP	$91.34^{(\pm 1.7e-3)}$	$91.49^{(\pm 1.8e-3)}$	$89.93^{(\pm 8.9e-3)}$	$89.93^{(\pm 7.3e-3)}$	$56.07^{(\pm 1.2e-2)}$	$56.71^{(\pm 7.6e-3)}$
	$91.33^{(\pm 1.8e-3)}$	$91.48^{(\pm 1.5e-3)}$	$89.94^{(\pm 9.1e-3)}$	$90.39^{(\pm 6.8e-3)}$	$56.13^{(\pm 1.2e-2)}$	$57.50^{(\pm 1.0e-2)}$
mPLUG-Owl	$82.90^{(\pm 1.9e-3)}$	$83.26^{(\pm 2.6e-3)}$	$88.41^{(\pm 3.9e-3)}$	$88.9^{(\pm 2.8e-3)}$	$75.94^{(\pm 6.2e-3)}$	$77.04^{(\pm 5.8e-3)}$
	$82.87^{(\pm 2.7e-3)}$	$83.56^{(\pm 3.1e-3)}$	$88.55^{(\pm 3.7e-3)}$	$89.87^{(\pm 2.3e-3)}$	$76.11^{(\pm 5.8e-3)}$	$78.61^{(\pm 7.9e-3)}$

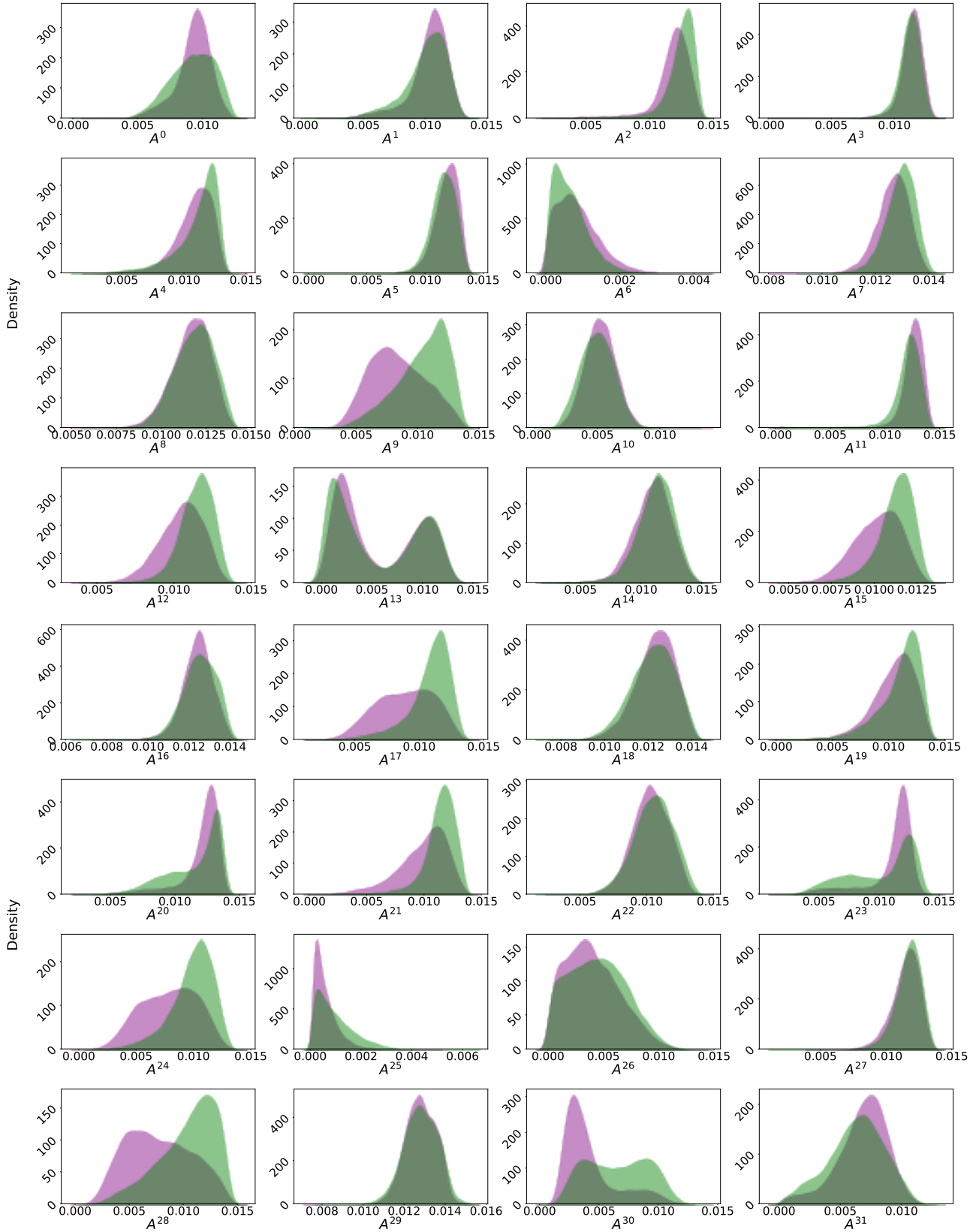


Figure 8. **Attention Metrics.** Visualization of the attention metrics Eq. (5) defined in Sec. 3.2 for **true** and **hallucinated** objects.